JMEPEG (2011) 20:1678–1683
DOI: 10.1007/s11665-011-9834-2

1059-9495/$19.00

Influence of Step Annealing Temperature on the Microstructure and Pitting Corrosion Resistance of SDSS UNS S32760 Welds

M. Yousefieh, M. Shamanian, and A. Saatchi

(Submitted June 12, 2010; in revised form December 13, 2010)

In the present work, the influence of step annealing heat treatment on the microstructure and pitting corrosion resistance of super duplex stainless steel UNS S32760 welds have been investigated. The pitting corrosion resistance in chloride solution was evaluated by potentiostatic measurements. The results showed that step annealing treatments in the temperature ranging from 550 to 1000 °C resulted in a precipitation of sigma phase and Cr_2N along the ferrite/austenite and ferrite/ferrite boundaries. At this temperature range, the metastable pits mainly nucleated around the precipitates formed in the grain boundary and ferrite phase. Above 1050 °C, the microstructure contains only austenite and ferrite phases. At this condition, the critical pitting temperature of samples successfully arrived to the highest value obtained in this study.

Keywords corrosion, microstructure, stainless steel, step annealing heat treatment, welding

1. Introduction

Super duplex stainless steels (SDSSs) are two-phase iron-based alloys consisting of ferrite (α) and austenitic (γ) phases. The ratio of both phases is typically 50:50. SDSSs have found widespread use in many industries such as oil and gas, petrochemical and chemical processing. The popularity of SDSSs is attributed to an attractive combination of high-corrosion resistance, excellent mechanical properties, good weldability and also a relatively low cost compared to other higher performance materials, such as super austenitic stainless steels and Ni-base alloys. During welding and subsequent heat treatment, several transformations take place in the heat-affected zone and in the weld metal. The best general properties of SDSS are obtained when the ferrite-austenite ratio is close to 50:50 (Ref 1), and other phases, such as chromium nitrides (Cr_2N), sigma (σ), secondary austenite (γ_2), and tertiary austenite (γ_3) are not present. The nucleation and growth processes of deleterious phases have been studied by many authors (Ref 2-7).

In general, it is difficult to avoid the formation of deleterious phases such as σ, γ_2, γ_3, and Cr_2N during welding and subsequent cooling and reheating passes. In fact, very low-heat inputs lead to high-ferrite contents and intense chromium nitride precipitation. On the other hand, high-heat inputs and/or long-time exposures to temperatures ranging from 550 to 1050 °C may cause precipitation of brittle intermetallic phases such as σ (Ref 8). Because of the complex alloying of the SDSS, a number of precipitation reactions can occur at temperatures below 1050 °C. All of these precipitation reactions are time and temperature-dependent. The presence of precipitates in the microstructure can deteriorate the corrosion resistance of the SDSS welds. Therefore, the precipitates should be eliminated by postweld heat treatment. In this regard, an annealing process may be necessary to eliminate the intermetallic precipitates such as Cr_2N, σ, γ_2, and γ_3.

During the recent years, the influence of annealing heat treatment on the corrosion resistance and mechanical properties of duplex and SDSSs have been studied (Ref 9-15). However, the information on the effect of step annealing on the pitting corrosion resistance of SDSS welds is scant.

The high-annealing temperatures necessary to eliminate σ in weld metal are not always desirable from a corrosion resistance point of view because α retains too much nitrogen in solution. Quenching from 1120 to 1150 °C can result in some nitride precipitation. To prevent this, a step annealing procedure can be applied. This article deals with the investigation of the influence of step annealing on the pitting corrosion resistance of SDSS (UNS S32760) welds in chloride solution by critical pitting temperature (CPT) measurements, which is more sensitive and reliable than other pitting-related methods such as pitting potential approach (Ref 16-18).

2. Materials and Experimental Method

A 5.0-mm thick, 500-mm diameter pipe made of super duplex UNS S32760 stainless steel was welded using gas tungsten arc welding (GTAW) process. The joints were prepared by machining to 75° groove angles. GTAW uses a nonconsumable tungsten electrode and an inert gas for arc shielding. In this process, an electric arc is formed between a tungsten electrode and the base metal. The arc region is

M. Yousefieh, M. Shamanian, and **A. Saatchi**, Department of Materials Engineering, Isfahan University of Technology, Isfahan 84156-83111, Iran. Contact e-mails: m.yousefieh@ma.iut.ac.ir and shamanian@cc.iut.ac.ir.

protected by an inert gas such as argon or helium. In this study, the protective gas was 99.99% pure argon (25 CHF and 40 CHF flow rate for backing and shielding). The welding parameters were controlled in order to maintain the heat input in the range of 0.5-2.0 kJ/mm for the root and the subsequent filler passes. The welding process parameters are summarized in Table 1. The chemical compositions of the base metal and filler metal are shown in Table 2. Commercial filler metals were chosen in this work for the sake of availability and adequacy of actual industrial procedures. GTAW filler metals contain copper additions to improve corrosion resistance.

Then, the weldments were subjected to step annealing heat treatment. In this procedure, the samples were maintained at 1150 °C to dissolve all σ formed during heating. Then, they were furnace cooled to different temperatures ranging from 550 to 1100 °C. Finally, the samples were quenched in water after 15 min holding at this temperature range. The step annealing heat treatment is schematically illustrated in Fig. 1.

Volumetric fractions of deleterious phases in welded samples were determined by quantitative metallography using Image Tool software (Ref 19). Before microstructural examination, the samples were ground, polished and then electrochemically etched in a KOH solution (100 mL H_2O + 15 g of potassium hydroxide), at a potential of 3 V for 12 s. This reagent was used to reveal σ and other deleterious phases, such as γ_2, γ_3 and eventually Cr_2N precipitated in association with σ (Ref 20, 21).

The microstructural investigations were performed using a scanning electron microscope (SEM) equipped with an energy dispersive x-ray (EDX) spectrometer for microanalysis. The x-ray count rate was estimated to be about 2×10^3 counts per second (cps).

The corrosive media, 1 mol/L NaCl, was made up of analytical grade reagent and distilled water. All the electrochemical measurements were carried using an EG&G-263A potentiostat. The tests were conducted in a conventional three-electrode cell, with Pt foil as the auxiliary electrode, and a saturated calomel electrode (SCE) as the reference electrode. The working electrode was constructed using the heat-treated samples embedded in epoxy resin with an exposure area of 1 cm^2, with a copper wire providing electrical contact. Prior to each CPT measurement, the working electrodes were ground and polished with 0.1 μm alumina paste, degreased with alcohol and cleaned in water. In order to avoid crevice corrosion, the interfaces between sample and resin were sealed with special silica gel sealant and then dried in the air. It should be noted that the occurrence of crevice corrosion after CPT tests means that the test results are invalid and must be discarded. The potentiostatic measurements were performed to obtain the CPT by applying an anodic potential of 750 mV_{SCE} and the solution temperature increased at a rate of (1 ± 0.3) °C/min until stable pitting occurred. The corresponding current density was recorded simultaneously with increasing the temperature throughout the test. The experiment was stopped when the current density reached 100 μA/cm^2 and kept surging for 1 min. The CPT was defined as the temperature where the current density is equal to 100 μA/cm^2 (Ref 11, 22). The test solution was bubbled with pure nitrogen gas (N_2) to get rid of oxygen gas (O_2) throughout the whole test (Ref 11). The CPT measurements were performed for at least five times on each sample in order to assure its repeatability. After the CPT measurements, the initiation sites of pitting corrosion were investigated by SEM.

Table 1 Welding parameters

Current, A	Voltage, V	Travel speed, mm/s	Heat input, kJ/mm
110	15	110	0.90

3. Results and Discussion

3.1 Influence of Different Step Annealing Procedures on the Microstructure

Figure 2 shows the microstructures of as-weld samples and those obtained by step annealing treatment at different temperatures. The microstructure of SDSS in the as-welded condition is shown in Fig. 2(a). It is clear σ phase is present at the α/γ interfaces, which are considered as preferential nucleation sites for the heterogeneous precipitation of intermetallic compounds. The σ precipitation is confirmed by the EDX analysis of the white region in Fig. 2(a), as illustrated in Table 3, which is the result of high-heat input and slow cooling rate under welding conditions. The σ volume fraction was about 32% in this sample.

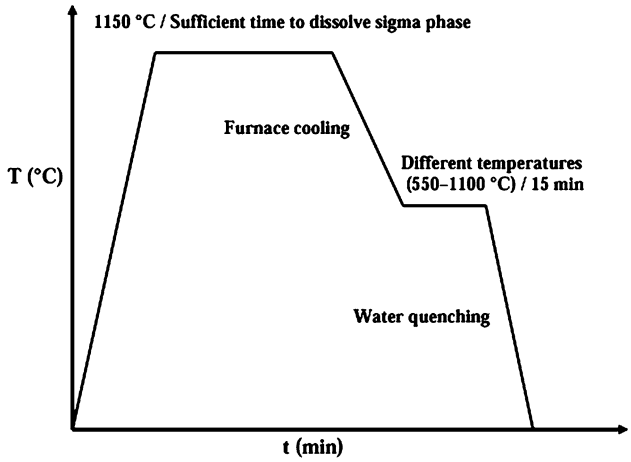

Fig. 1 Schematic illustration of the step annealing heat treatment

Table 2 Chemical composition of the base and filler materials (wt.%)

Element	C	Mn	P	S	Si	Cr	Ni	Mo	N	Cu
Base metal (UNS S32760)	0.03	0.82	0.02	0.01	0.93	23.2	6.3	3.0	0.23	0.61
Filler metal (ER 2594)	0.03	0.73	0.001	0.002	0.94	23.1	9.2	3.0	0.22	0.54

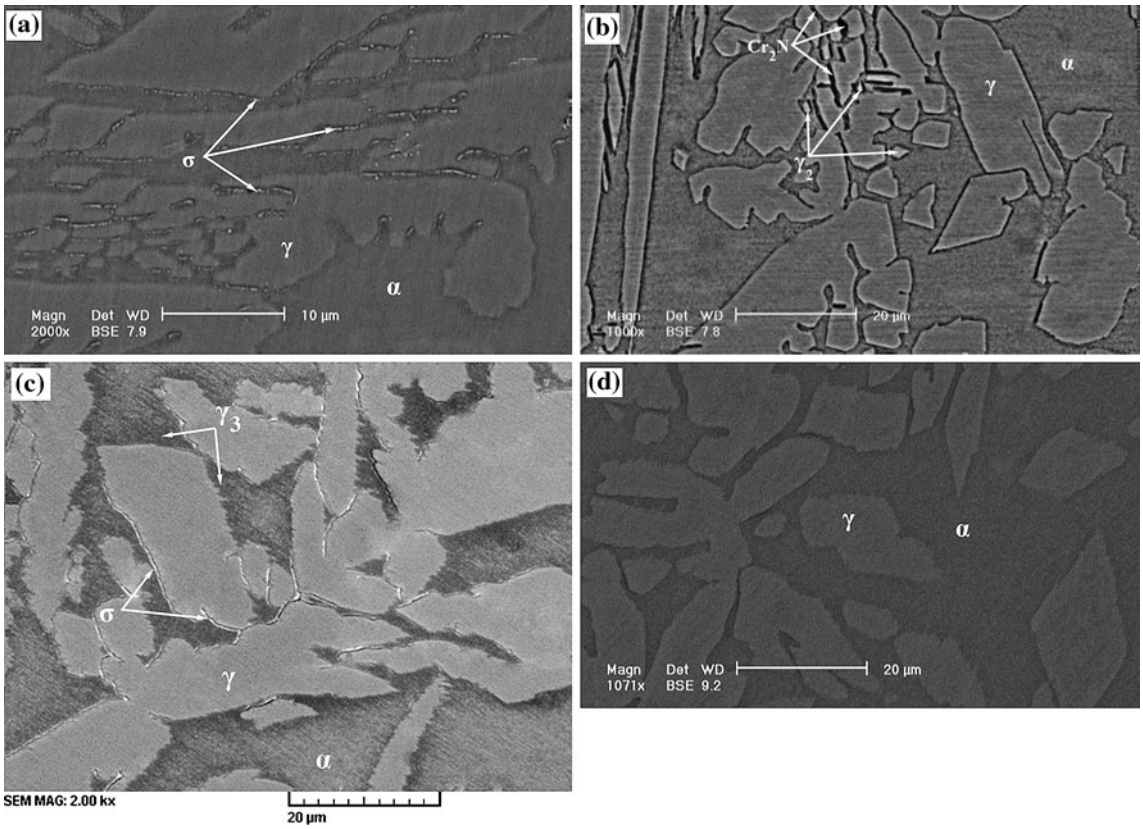

Fig. 2 SEM micrographs of samples (a) for as-welded condition, (b) step annealed at 700 °C for 15 min, (c) step annealed at 850 °C for 15 min, and (d) step annealed at 1050 °C for 15 min

Table 3 EDX analysis (wt.%) of different phases present in the different condition

		Element			
Treatment condition	**Phase**	**Fe**	**Cr**	**Mo**	**Ni**
As-welded sample	σ	58.9	31.2	5.8	4.1
Step annealed/700 °C/15 min	γ_2	68.7	20.8	1.9	8.6
Step annealed/850 °C/15 min	σ	57.5	32.4	6.2	3.9
Step annealed/850 °C/15 min	γ_3	76.61	15.2	0.39	7.8

When the step annealing process was applied at temperatures between 550 and 750 °C, the precipitates formed in the α/γ interfaces and α/α interfaces were high in chromium content. Meantime, the lighter region near the precipitates showed lower chromium content regions as compared to other phases, i.e., α phase, γ phase, and precipitates. The low-chromium region is called γ_2 phase (Ref 23, 24) (as illustrated in Table 3). As shown in Fig. 2(b), it is clear that the high chromium-containing precipitates formed in the α/γ interfaces and α/α interfaces were Cr_2N, which also resulted in the formation of low chromium-containing γ_2. The EDX analysis showed that the content of chromium in Cr_2N reached up to 76.2 wt.%. As the step annealing temperature increases, the amount of Cr_2N precipitates increased drastically along the α/γ interfaces and α/α interfaces.

After step annealing between 800 and 1000 °C, the precipitation of σ phase occurs at the α/γ interfaces, as shown in Fig. 2(c). The σ phase is formed in iron and chromium binary system. The formation of σ phase in SDSS is described by the decomposition of α through an eutectoid transformation ($\alpha \rightarrow \sigma + \gamma_3$). After the nucleation process, σ phase particles grow into the adjacent α grains. The preferential precipitation of σ phase from α is due to the chromium and molybdenum enrichment of α phase (Ref 25). In fact, the precipitation of the intermetallic σ phase is accompanied by the formation of a new austenitic phase (tertiary austenite; γ_3). As the σ phase forms, these particles enrich in chromium and molybdenum and simultaneously nickel diffuses into α (Ref 26). The presence of the σ and γ_3 precipitates was confirmed by EDX, as shown in Table 3.

Figure 2(d) shows a SEM micrograph of the sample step annealed at 1050 °C. As seen in this figure, the microstructure consists of only α and γ. It means that precipitates or intermetallic phases are not present.

3.2 Influence of Different Step Annealing Temperature on the Pitting Corrosion Resistance

Figure 3 shows the typical curves of current density against temperature for samples step annealed at different temperatures for 15 min. It was concluded that the current density exhibited a lower value less than 1 μA/cm^2 during the initial heating, suggesting that SDSS was protected by the passive film on the surface. As temperature increased and approached to CPT, some current density fluctuations were observed below the CPT, which were associated to breakdown of passive films in the form of metastable pits. As the temperature reached to the CPT, the current density continuously increased due to the formation of the stable pits.

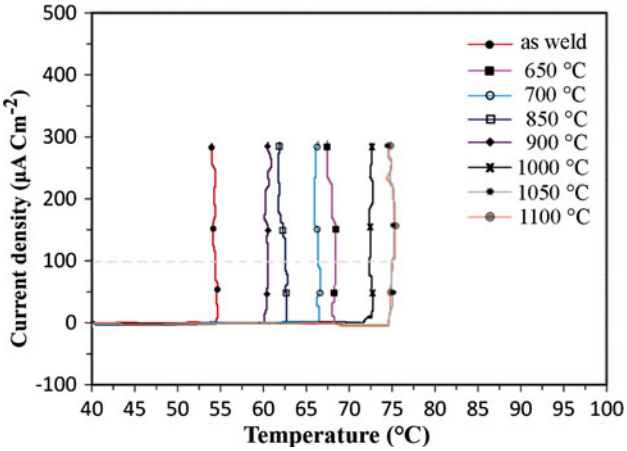

Fig. 3 Typical curves of current density and temperature for SDSS UNS S32760 welds in 1 mol L^{-1} NaCl solution step annealed at different temperatures for 15 min at a potential of 750 mV_{SCE}

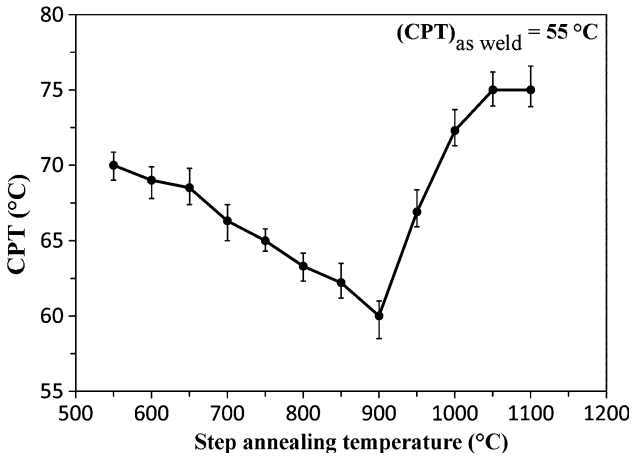

Fig. 4 CPT of samples step annealed at different temperatures for 15 min

Figure 4 shows the effect of step annealing temperature on the CPT. The CPT value of the as-welded sample was 55 °C, which is the lowest value among the all CPT values in this study. As the step annealing temperature increased from 550 to 750 °C, the CPT decreased from 70 to 65 °C due to the precipitation of Cr_2N at the α/α and α/γ sub-grain boundaries. At this temperature range (550-750 °C), an intense Cr_2N precipitation reaction occurs on cooling since the nitrogen content in α is higher than solubility limit of nitrogen in α (Ref 5). According to the EDX analysis, the content of chromium in Cr_2N reached up to 76.2 wt.%, resulting in the formation of localized depletion areas Cr around the Cr_2N. This Cr-depletion zones became unstable and transformed into γ_2, leading to the decrease of CPT values. It can be inferred from these results that the deleterious effect of Cr_2N on pitting corrosion is associated to the formation of Cr-depletion zone adjacent to Cr_2N precipitates.

As the step annealing temperature further increased to 900 °C, the CPT of step annealed sample decreased to the minimum value of 60 °C. Whereas the CPT decreased when the step annealing temperature continued to increase, mainly owing to the precipitation of higher volume fraction of σ phase. The minimum CPT (among the step annealed samples) was obtained when the samples were step annealed at 900 °C, which means that the samples step annealed at 900 °C had the minimum pitting corrosion resistance. The enrichment of α in γ stabilizing elements and the loss of α stabilizing elements lead to an unstable ferrite, transforming into an austenitic phase (γ_3) (Ref 26). This austenite is depleted in chromium and molybdenum, leading to the minimum value of CPT. EDX measurements showed that chromium content is reduced from 23 to 9% and a nearly total loss of molybdenum. Calculations of Kobayashi and Wolynec have shown that as the chromium content of the γ_3 falls below 11%, the phase becomes prone to pitting corrosion (Ref 4, 26). As step annealing temperature increased over 900 °C, the CPT began to increase. It can be attributed to decrease in amount of intermetallic precipitates from 17 to less than 10%.

It should be noted that when step annealing temperature was higher than 1050 °C, the CPT of samples gradually reached to a steady value of about 75 °C.

From the SEM micrographs, EDX analysis and CPT measurements, it can be deduced that the presence of intermetallic precipitates in SDSS welds strongly affects the corrosion performance. The precipitation of brittle phases leads to the loss of corrosion resistance. This is in agreement with the result of previous studies on duplex stainless steels (Ref 26, 27).

3.3 Pit Morphology

The morphology of pits on the surface of samples after CPT measurements was investigated by SEM. Typical morphologies of the metastable pit are shown in Fig. 5. Figure 5(a) shows the as-welded sample investigated just after the CPT measurement. The metastable pits with diameter of ~5 μm were seen to be initiated around the σ phase in the α/γ interface, due to the presence of chromium-depleted region around the σ phase at the α/γ boundary.

Figure 5(b) shows the metastable pits with diameter of ~4 μm formed on the sample step annealed at 700 °C for 15 min. It seems that the pits are first initiated around the Cr_2N and γ_2 at the α/γ and α/α boundaries and then propagate in α phase. γ_2 had lower Cr content than α and γ phases, leading to reduce pitting corrosion resistance (Ref 24).

Figure 5(c) illustrates the typical metastable pit with diameter of 4 μm formed on the sample step annealed at 850 °C for 15 min after CPT measurement. At this condition, pits preferentially nucleated around σ and γ_3 formed in the α/γ interface. The distinctive mechanism of pitting corrosion for this sample was the selective dissolution of γ_3 phase, because the γ_3 was used as a path for the corrosive environment to permeate from the outer surface to the inside of the samples.

Most of the metastable pits of sample step annealed at 1050 °C were located at α phase, as shown in Fig. 5(d). This could be explained with the different chemical composition of phases, namely the pitting resistance equivalent number (PREN) of the two phases (Ref 28). The alloy (or phase) with higher PREN exhibits better pitting corrosion resistance (Ref 11). The PREN in the sample step annealed at 1050 °C was calculated using the formula (PREN = wt.%Cr + 3.3 wt.%Mo + 20 wt.%N) (Ref 29) with the data listed in Table 4. It should be noted that the nitrogen content in ferrite is taken as the saturation value (≈0.05%), and the rest partitions to austenite (Ref 24). Based on this formula, the PREN of ferrite ($PREN_\alpha$ = 35.97) phase was lower than that of austenite phase ($PREN_\gamma$ = 37.98), which means that the pits mainly initiated in α phase.

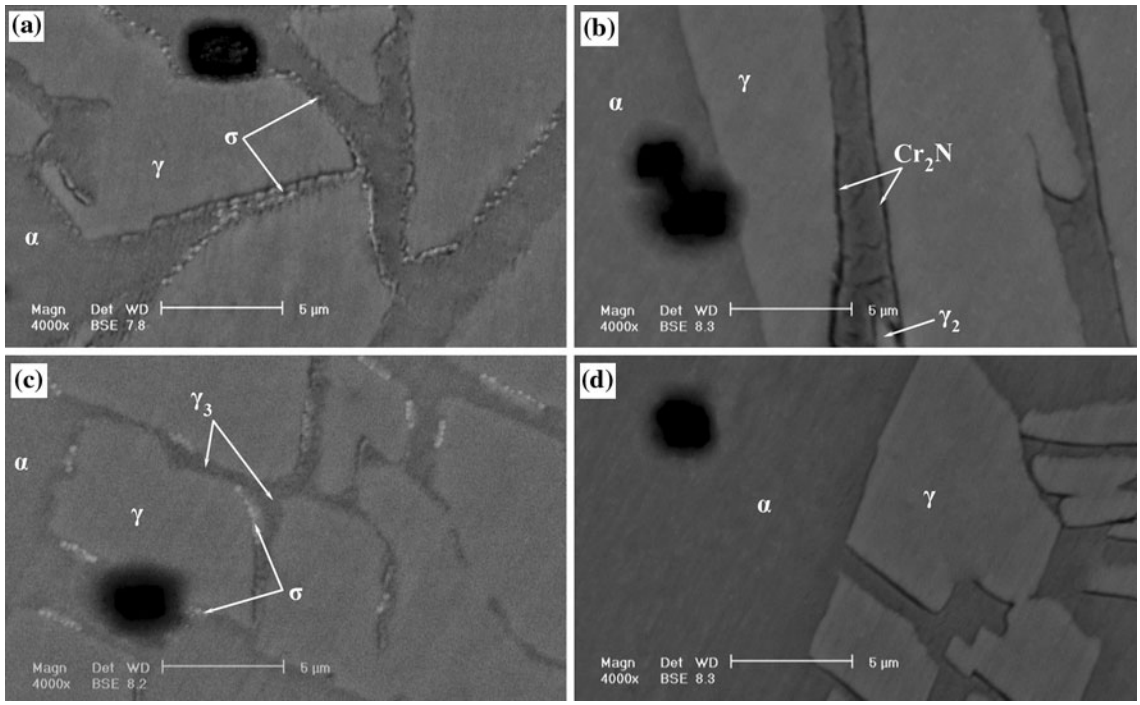

Fig. 5 The metastable pits and corrosion attack on the SDSS UNS S32760 welds observed just after the CPT measurement, characterized by SEM (a) as-welded sample, (b) step annealed at 700 °C for 15 min, (c) step annealed at 850 °C for 15 min, and (d) step annealed at 1050 °C for 15 min

Table 4 The chemical composition (wt.%) and PREN of ferrite and austenite in the samples step annealed at 1050 °C for 15 min

Step annealing temperature, °C	Phase	Element				PREN
		Cr	Mo	Ni	N	
1050	Austenite	22.27	2.64	8.64	0.35	37.98
	Ferrite	24.02	3.32	5.81	0.05	35.97

4. Conclusions

In this study, the influence of step annealing heat treatment on the pitting corrosion resistances of SDSS (UNS S32760) welds was investigated in chloride solution. The conclusions drawn from this study are summarized as follows:

- GTAW process of super duplex stainless UNS S32760 using ER 2594 filler metal resulted in a significant variation in the microstructure compared to the base material. Higher amounts of σ phase were found in the as-welded sample, leading to a rapid reduction of the pitting corrosion resistance.
- The pitting corrosion resistance of super duplex stainless UNS S32760 welds is intensely affected by the step annealing temperature. When step annealing temperature was higher than 1050 °C, the CPT of samples gradually reached to a steady value of about 75 °C, which is the highest value obtained in the present study. At this condition, precipitates or intermetallic phases were not observed in the microstructure. The metastable pits were mainly initiated in α phase for samples step annealed at temperatures above 1050 °C, because the PREN of austenite phase ($PREN_\gamma = 37.98$) was higher than that of ferrite phase ($PREN_\alpha = 35.97$).
- The step annealing treatment of UNS S32760 SDSS welds at temperatures below 1050 °C produced intermetallic precipitates such as Cr_2N and σ phases along the α/γ and α/α boundaries. These precipitates contained higher chromium or chromium/molybdenum content as compared to α and γ phases. Adjacent to the precipitates, a low-chromium or chromium/molybdenum region called γ_2 and γ_3 were found, respectively. The metastable pits were seen to be initiated around the precipitates formed in the α/γ and α/α boundaries for samples step annealed at temperatures below 1050 °C.
- A significant decrease in CPT occurs at 900 °C mainly due to precipitations of γ_3 phase. This austenite (γ_3) is depleted in chromium and molybdenum, leading to the minimum value of CPT among the step annealed samples ($CPT_{min.} = 60$ °C). Pit initiation was found to be around the precipitates due to the selective dissolution of the γ_3 phases.

References

1. V. Muthupandi, P. Bala Srinivasan, S.K. Seshadri, and S. Sundaresan, Effect of Weld Metal Chemistry and Heat Input on the Structure and Properties of Duplex Stainless Steels, *Mater. Sci. Eng. A*, 2003, **358**, p 9–16
2. R.N. Gunn, *Duplex Stainless Steels—Microstructure Properties and Applications*, Abington Publishing, Cambridge, 2003
3. K.M. Lee, H.S. Cho, and D.C. Chjoi, Effect of Isothermal Treatment of SAF 2205 Duplex Stainless Steel on Migration of δ/γ Interface Boundary and Growth of Austenite, *J. Alloys Compd.*, 1999, **285**, p 156–161

4. D.Y. Kobayashi and S. Wolynec, Evaluation of the Low Corrosion Resistant Phase Formed During the Sigma Phase Precipitation in Duplex Stainless Steels, *Mater. Res.*, 1999, **2**(4), p 239–247
5. J.C. Lippold and D.J. Kotecki, *Welding Metallurgy and Weldability of Stainless Steels*, John Wiley & Sons, New York, 2005
6. J.O. Nilsson, Super Duplex Stainless Steels, *Mater. Sci. Technol.*, 1992, **8**, p 685–700
7. A.J. Ramirez, J.C. Lippold, and S.D. Brandi, The Relationship Between Chromium Nitride and Secondary Austenite Precipitation in Duplex Stainless Steels, *Met. Mater. Trans. A*, 2003, **34**, p 1575–1597
8. S.S.M. Tavares, J.M. Pardal, L.D. Lima, I.N. Bastos, A.M. Nascimento, and J.A. de Souza, Characterization of Microstructure, Chemical Composition, Corrosion Resistance and Toughness of a Multipass Weld Joint of Superduplex Stainless Steel UNS S32750, *Mater. Charact.*, 2007, **58**, p 610–616
9. L. Duprez, B.D. Cooman, and N. Akdut, Microstructure Evolution During Isothermal Annealing of a Standard Duplex Stainless Steel Type 1.4462, *Steel Res.*, 2000, **71**, p 417–422
10. C.J. Park and H.S. Kwon, Electrochemical Noise Analysis of Localized Corrosion of Duplex Stainless Steel Aged at 475 °C, *Mater. Chem. Phys.*, 2005, **91**, p 355–360
11. H. Tan, Y. Jiang, B. Deng, T. Sun, J. Xu, and J. Li, Effect of Annealing Temperature on the Pitting Corrosion Resistance of Super Duplex Stainless Steel UNS S32750, *Mater. Charact.*, 2009, **60**, p 1049–1054
12. L. Zhang, W. Zhang, Y. Jiang, B. Deng, D. Sun, and J. Li, Influence of Annealing Treatment on the Corrosion Resistance of Lean Duplex Stainless Steel 2101, *Electrochim. Acta*, 2009, **54**, p 5387–5392
13. W. Zhang, L. Jiang, J. Hu, and H. Song, Effect of Ageing on Precipitation and Impact Energy of 2101 Economical Duplex Stainless Steel, *Mater. Charact.*, 2009, **60**, p 50–55
14. F. Shi, L.J. Wang, W.F. Cui, and C.M. Liu, Precipitation Behavior of M_2N in a High-Nitrogen Austenitic Stainless Steel During Isothermal Aging, *Acta Metall. Sin. (Engl. Lett.)*, 2007, **20**(2), p 95–101
15. B. Deng, Z. Wang, Y. Jiang, H. Wang, J. Gao, and J. Li, Evaluation of Localized Corrosion in Duplex Stainless Steel Aged at 850 °C With Critical Pitting Temperature Measurement, *Electrochim. Acta*, 2008, **54**, p 2790–2794
16. B. Deng and Y. Jiang, Dependence of Critical Pitting Temperature on the Concentration of Sulphate Ion in Chloride-Containing Solutions, *Appl. Surf. Sci.*, 2007, **253**, p 7369–7375
17. M.H. Moayed and N.J. Laycock, Dependence of the Critical Pitting Temperature on surface roughness, *Corros. Sci.*, 2003, **45**, p 1203–1216
18. R. Ovarfort, Critical Pitting Temperature Measurements of Stainless Steels With An Improved Electrochemical Method, *Corros. Sci.*, 1989, **29**, p 987–993
19. Image Tool Version 3.0, University of Texas Health Science Center at San Antonio, Free Software, Available in http://ddsdx.uthscsa.edu/dig/itdesc.html. Accessed 9.3.2007
20. J.M. Pardal, S.S.M. Tavares, M. Cindra Fonseca, J.A. De Souza, R.R.A. Côrte, and H.F.G. De Abreu, Influence of the Grain Size on Deleterious Phase Precipitation in Superduplex Stainless Steel UNS S32750, *Mater. Charact.*, 2009, **60**, p 165–172
21. C.J. Park, H.S. Kwon, and M.M. Lohrengel, Micro-Electrochemical Polarization Study on 25% Cr Duplex Stainless Steel, *Mater. Sci. Eng. A*, 2004, **372**, p 180–185
22. Standard Test Method for Electrochemical Critical Pitting Temperature Testing of Stainless Steels, Designation, p 150–199
23. M.E. Wilms, V.J. Gadgil, J.M. Krougmen, and F.P. Ijsseling, The Effect of σ-Phase Precipitation at 800 °C on the Corrosion Resistance in Sea-Water of a High Alloyed Duplex Stainless Steel, *Corros. Sci.*, 1994, **36**, p 877–881
24. L. Zhang, Y. Jiang, B. Deng, W. Zhang, J. Xu, and J. Li, Effect of Aging on the Corrosion Resistance of 2101 Lean Duplex Stainless Steel, *Mater. Charact.*, 2009, **60**, p 1522–1528
25. R. Badji, M. Bouabdallah, B. Bacroix, C. Kahloun, B. Belkessa, and H. Maza, Phase Transformation and Mechanical Behavior in Annealed 2205 Duplex Stainless Steel Welds, *Mater. Charact.*, 2008, **59**, p 447–453
26. M. Pohl, O. Storz, and T. Glogowski, Effect of Intermetallic Precipitations on the Properties of Duplex Stainless Steel, *Mater. Charact.*, 2007, **58**, p 65–71
27. V.S. Moura, L.D. Lima, J.M. Pardal, A.Y. Kina, R.R.A. Corte, and S.S.M. Tavares, Influence of Microstructure on the Corrosion Resistance of the Duplex Stainless Steel UNS S31803, *Mater. Charact.*, 2008, **59**, p 1127–1132
28. G. Lothongkum, P. Wongpanya, S. Morito, T. Furuhara, and T. Maki, Effect of Nitrogen on Corrosion Behavior of 28Cr-7Ni Duplex and Microduplex Stainless Steels in Air-Saturated 3.5% NaCl Solution, *Corros. Sci.*, 2006, **48**, p 137–153
29. L. Weber and P.J. Uggowitzer, Partitioning of Chromium and Molybdenum in Duplex Stainless Steels With Respect to Nitrogen and Nickel Content, *Mater. Sci. Eng. A*, 1998, **242**, p 222–229